TÜBİTAK

Turk J Phys
34 (2010) , 83 – 96.

doi:10.3906/fiz-0908-42

Influence of the nitrogen concentration on the electrical characteristic of hydrogenated amorphous silicon nitride (a-SiN$_x$:H) based Schottky diodes

İlker AY[1] **and Hüseyin TOLUNAY**[2]
[1] *Hacettepe University, Bala Higher School of Vocational Education*
06720 Bala, Ankara-TURKEY
e-mail: ilkeray@hecettepe.edu.tr
[2] *Department of Physics Engineering, Hacettepe University*
06800-Beytepe, Ankara-TURKEY
e-mail: htolunay@hacettepe.edu.tr

Received 27.08.2009

Abstract

In this study, the Schottky diode characteristic of hydrogenated amorphous silicon nitride (a-SiN$_x$:H) samples containing various amounts of nitrogen have been investigated via both I-V and C-V measurements. From forward bias I-V measurements in the dark, the barrier height of samples (ϕ_{B0}), ideality factor (η), modified Richardson constant (A*) and series resistances (R_s) have been obtained as the function of temperature for different nitrogen content. In addition, forward and reverse bias current ratios (I_f / I_r) at $V = 1$ volt have been investigated as the function of temperature for different nitrogen content. Light sensitivity of the samples has also been investigated under different light intensities at room temperature.

From the C-V measurements in the dark and at room temperatures, the dielectric constant of each samples have been obtained as a function of nitrogen content.

Key Words: a-SiN$_x$:H, Schottky diodes, I-V characteristics, ohmic contact, C-V measurements

1. Introduction

Silicon nitride (SiN$_x$) plays an essential role in the making of silicon based semiconductor devices. Generally, due to the fact that its impurity is a good barrier against diffusion and that the dielectric constant is likely to change, it is used as the gate in thin film transistors and as insulating materials in MIS (Metal-Insulator-Semiconductor) structure [1–5]. It is also used as mask against oxidation on the silicon surface and

load devices in memory apparatuses. The most important reason behind silicon nitride's popularity is its ability to raise apparatus productivity, high deposition speed, homogeneously deposition and low cost.

In this study, the Schottky diode characteristic of hydrogenated amorphous silicon nitride (a-SiN_x:H) samples containing various amounts of nitrogen (Table 1) have been studied by both taking current-voltage (I-V) measures through a wide temperature range (420–145 K) in the dark and capacitance-voltage (C-V) measures at room temperature.

A Keithley 6430 source meter was used for I-V measurements of the samples while the temperature was controlled by a Cryodial ML 1400A temperature controller and read by an Agilent 34401A digital multimeter.

Out of the forward bias I-V measurements in the dark, the barrier height (ϕ_{B0}) of samples, ideality factor (η), modified Richardson constant (A^*) and series resistances (R_s) have been obtained as the function of temperature for different nitrogen content. Also, forward and reverse bias current ratios (I_f/I_r) at V=1 volt have been investigated as the function of temperature for different nitrogen content. The light sensitivity of the samples which were prepared in different nitrogen content has been investigated by I-V measurements under different light intensities at room temperature.

The variation of dielectric constant with respect to the nitrogen content has been obtained with HP 4192A LF impedance analyzer and C-V measuring on $0.1V_{tt}$ and 1 MHz fixed frequency.

2. Experimental method

It was showed by many researchers that the lowest series resistance and the lowest barrier height in a-Si:H/metal structures were produced by Mg [6–9]. We also used Mg with reference to these sources as the back metal electrode. For the upper electrode, we used Au.

a-SiN_x:H films with different nitrogen content were prepared by decomposition of SiH_4-NH_3 gas mixture in the RF glow discharge system. Before deposition of a-SiN_x:H films, back contact of samples was deposited on corning 7059 substrates (9×11 mm^2) using a high vacuum thermal evaporation system. Before evaporation, substrates were heated to a suitable temperature for better adhesion to the surface of Mg which is between 250 °C – 300 °C. After having substrates reached to a suitable temperature, the Mg was evaporated. An identical a-SiN_x:H film was deposited on these back contacts at 230 °C substrate temperature (T_s). The other deposition parameters, such as the RF power and the total gas pressure were 6 W and 200 mTorr, respectively. The different nitrogen content of the samples were determined with parameter r which is obtained from the relative partial pressure of SiH_4 and NH_3 gases in the glow discharge system, defined by the ratio

$$r = \frac{P_{NH_3}}{P_{NH_3} + P_{SiH_4}}. \tag{1}$$

In order to form the Schottky barrier, Au was evaporated in spots the radius of 0.6 mm with high vacuum evaporation system by using suitable masks on a-SiN_x:H film. The name and nitrogen content of the prepared Mg / a-SiN_x:H / Au samples have been given in Table 1.

Before the I-V measurements all samples were annealed in the dark vacuum cryostat at 430 K for 30 minutes to remove the trapped carriers which are in the surface trapping centers and then I-V measurements were performed by using Keithley 6430 source meter in dark and constant temperature. During the I-V measurements, sample temperature was controlled by using Cryodial ML 1400A temperature controller for each temperature point.

Table 1. Preparation condition of a-SiN$_x$:H samples.

Samples	P_{NH_3} (mTorr)	P_{SiH_4} (mTorr)	r	T$_s$ (°C)	Deposition time (hour)
E1	-	200	0	230	2
H12	1	~ 200	0.005	230	2
F1	28	~ 172	0.14	230	2
G1	50	~ 150	0.25	230	2
J1	100	~ 100	0.50	230	2

Because of the high resistance of pure a-Si:H, Current-Voltage (I-V) measurements are the most reliable method for determining the barrier height of the Schottky diodes. As in the case of metal/crystalline semiconductor, in metal/amorphous semiconductor, there are four kinds of current mechanism to explain the current flow through the metal-semiconductor interface [10, 11] under forward bias. These mechanisms are thermionic emission (TE), tunneling, generation-recombination and leakage current. Thus, the total current is assumed to be the sum of all these currents. The total current is thus given by the relation

$$\begin{aligned} I &= I_{TE0}\left[\exp\left(\tfrac{q(V-IR_s)}{kT}\right)-1\right]+I_t\exp\left(\tfrac{q(V-IR_s)}{E_0}\right) \\ &\quad +I_{gr}\left[\exp\left(\tfrac{q(V-IR_s)}{2kT}\right)-1\right]+\tfrac{V-IR_s}{R_L} \end{aligned} \quad . \tag{2}$$

Here, R_s is series resistance, E_0 is a parameter dependent on the barrier transparency, R_L denotes the limits the ohmic part of the leakage current; and I_{TE0}, I_t, and I_{gr} are, respectively, the reverse bias saturation currents for the thermionic emission, tunneling and generation-recombination current contributions. Although there are four kinds of current mechanism, generally only one current mechanism is dominant for I-V measurement. Even if more than one current mechanism is dominant, some sections of the I-V curve can be separated according to the ideality factor and each region can be investigated by the dominant current mechanism. Hence, equation (2) is simplified by using the definition of η for $V > 2kT/q$ and the total current I can be written as [12]

$$I = I_0 \exp\left(\frac{q\,(V-IR_s)}{\eta kT}\right), \tag{3}$$

where I_0 is the reverse bias saturation current and η is the ideality factor.

For η=1, only TE current mechanism is dominant and barrier height independent of the bias. In this condition $I = I_{TE}$ and $I_0 = I_{TE0}$. Thermionic emission reverse bias saturation current is given as

$$I_{TE0} = SA^*T^2 \exp\left(-\frac{\phi_{B0}}{kT}\right), \tag{4}$$

where ϕ_{B0} is the barrier height; S is the diode area and A* denotes the modified Richardson constant which includes effective interface layer and uncertainty of contact area. For the above case, a graph of $\ln(I)$ as a function of V graphic is linear according to equation 3. Its slope gives q/kT and the intercept of the $\ln(I)$ axis gives I_{TE0}. If this condition is repeated under different temperatures, we can evaluate the ϕ_{B0} and A* from a plot of $\ln(I_{TE0}/T^2)$ versus $1/T$, according to equation 4.

If η varies between 1 and 2 ($1< \eta <2$), the tunneling current mechanism is dominant and intercept of the $\ln(I)$ axis gives the tunneling reverse bias saturation current (I_t). If η=2, the generation-recombination current mechanism is the dominant and we can find generation-recombination reverse bias saturation current (I_{gr}). If $\eta >2$, the leakage current mechanism is dominant. It is clear that if the temperature dependence of η is investigated with the use of I-V measurements, we can obtain good knowledge about the current mechanism.

In conclusion, the value of η is the most important parameter to be evaluated for a Schottky diode. For example, if barrier height is to be evaluated when $\eta \neq 1$, the result is not correct. Because saturation current determined for $\eta \neq 1$ is different from the correct I_{TE0} value. To overcome this problem, different regions of I-V curves are used according to their η values as suggested by Donoval. Hence the correct parameters of I_{TE0} are calculated using the η=1 region.

To calculate series resistance of diodes Cheung method [13] is used. According to Cheung method equation 3 can also be written

$$\frac{\mathrm{d}V}{\mathrm{d}(\ln(I))} = IR_S + \eta\frac{kT}{q}. \tag{5}$$

Equation 5 should give a straight line when plotted as a function of I. Thus the slope and intercept of the plot of $\mathrm{d}V/\mathrm{d}(\ln(I))$ versus I, gives R_s and $\eta kT/q$ respectively. If η=1 then equation 3 can be written

$$H(I) = IR_S + \frac{\phi_{B0}}{q} \tag{6}$$

where

$$H(I) = V - \frac{kT}{q}\ln\left(\frac{I}{SAT^2}\right). \tag{7}$$

In this case, plot of $H(I)$ as a function of I, according to Equation 6, also give a straight line. In addition, we can also find out the ϕ_{B0} from the intercept of the $H(I)$ axis.

3. Experimental results and discussion

The I-V graphs of the samples with different nitrogen content obtained in the dark and at the room temperature are shown in Figure 1. As district from crystal Schottky diodes, forward bias current of our samples have been saturated at $V \geq 1$ volt. It isn't surprising because of the fact that there is no orderly structure in amorphous structures and there are localize energy level in the optical band gap. However small values of voltage ($V <1$ volt), our samples behaves like crystal Schottky diodes. So we can investigate the diodes parameters in this range for accordance to nitrogen content of samples. Localize energy levels in the optical band gap are behaves as deep-charge trapping centers. The density of these centers increased with increasing nitrogen concentration. Thus the diode characteristic is deteriorated with increasing nitrogen concentration. And it tends to be insulators.

As shown in Figure 1, for the small amounts of nitrogen, ($r \leq 0.14$), the forward bias current has little increase compared with the pure sample (a-Si:H). As the content of nitrogen increases ($r >0.14$) forward bias current decreases while reverse bias current increases and forward-reverse bias current ratio (I_f/I_r), at V=1 volt, decreases.

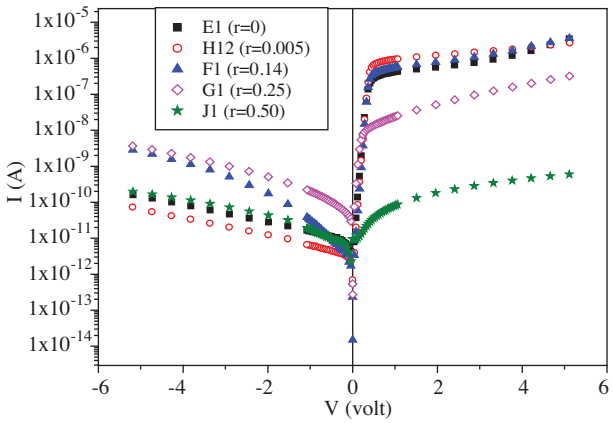

Figure 1. Current-Voltage characteristics of different nitrogen content a-SiN$_x$:H samples in the dark and at room temperature.

To calculate the Schottky diode characteristic of hydrogenated amorphous silicon nitride (a-SiN$_x$:H) samples that contain various amounts of nitrogen, samples have been characterized for their I-V behavior over a wide temperature range (420–145 K) in the dark. Temperature dependence of the I-V curve of the sample E1 is shown in Figure 2. As shown in Figure 2, both reverse and forward currents increased with temperature.

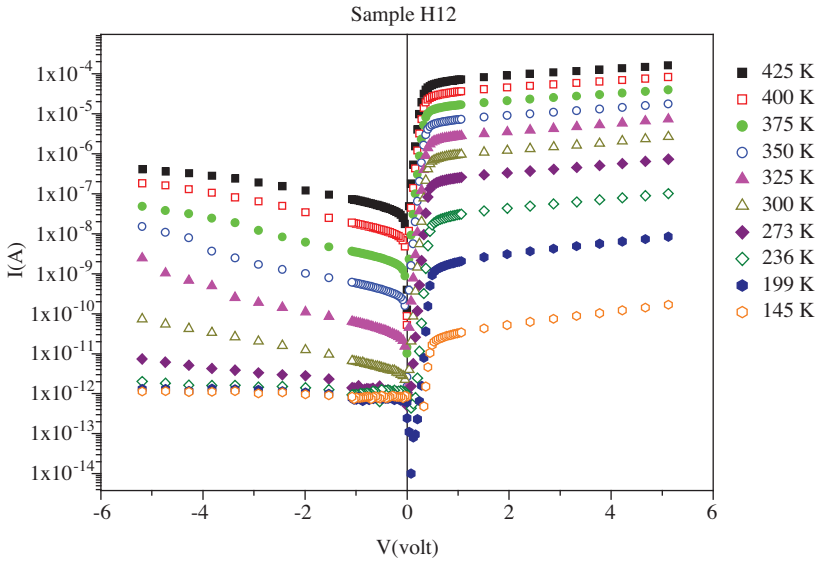

Figure 2. Temperature dependence of the I-V characteristics of sample H12 in the dark.

Also, the forward and reverse bias current ratio I_f / I_r at V=1 volt, calculated in accordance to with I-V measurements for a wide range of temperatures, shows Gaussian behavior for light nitrogen content alloys ($r \leq 0.25$) samples (Figure 3); however, as the nitrogen content is r=0.50 the I_f / I_r ratio does not change with the increasing temperature. In Figure 3, it is seen that I_f / I_r ratio recedes to 10^4 as nitrogen increases; in addition, the multiplying the I_f / I_r ratio with its multipliers is given in order to compare it with the other samples. At the same time, the temperature at which the inclination makes its peak, shifted to 250 K from

283 K as the nitrogen content becomes r=0.25. However, I_f / I_r ratio was decreased 500 times. As the nitrogen content is r=0.50 I_f / I_r ratio comes closer to 1 for all temperatures.

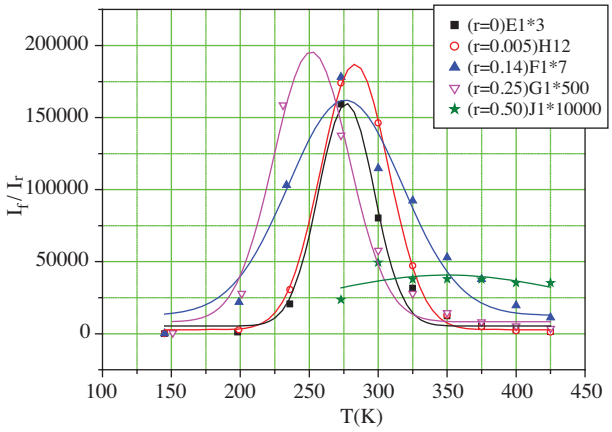

Figure 3. Temperature dependence of the forward and reverse bias current ratio (I_f / I_r) for samples with different nitrogen content. (The asterix * followed by a number denotes the multiplication factor.)

Having a look at the change of the ideality factor of the samples with respect to temperature, it has been observed that the dominant current mechanism over the room temperature is TE for samples nitrogenized as r$\leq$0.25 and (Figure 4). However, in lower temperatures, while field emission (FE) is dominant in some samples, in others thermionic field emission (TFE) is dominant. In the r=0.50 case, the sample acted as insulator and has shown no diode behavior.

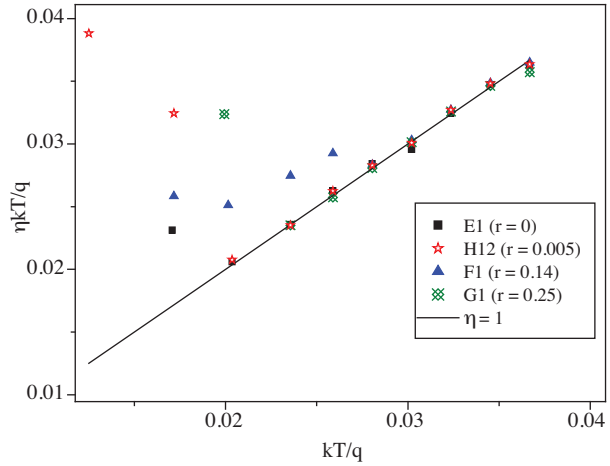

Figure 4. Temperature dependence of the ideality factor for samples with different nitrogen content.

In amorphous structures, it is known that the modified Richardson constant is an important parameter when calculating barrier height. Figure 5 shows a graph of $\ln(I_{TE0}/T^2)$ against $1000/T$ for $r \leq 0.25$ lightly nitrogen content alloy samples. The barrier height and modified Richardson constant calculated from the Figure 5 have been given in Table 2. The temperature dependence of the barrier height of sample has been calculated using Equation 4 for two Richardson constants. The first is modified as Richardson constant which

was calculated from a plot of $\ln(I_{TE0}/T^2)$ versus $1000/T$. Here, I_{TE0} has been found where ideality factor is kept 1 or close to 1 by using a plot of $\ln(I)$ versus V. The second Richardson constant is taken from literature for n-type crystal Si semiconductor. These calculations cannot be performed for the r=0.50 highly nitrogen content alloy sample due to the insulating behavior. As found in Figure 6, the barrier height, which was calculated by using modified Richardson constant in Equation 4, each sample has not changed with temperature. However, the barrier height calculated by the taken Richardson constant from the literature for n-type crystal Si semiconductor has decreased as the temperature decreases and it intersects with the barrier height calculated for modified Richardson constant at zero Kelvin. The barrier height also increases at low nitrogen content while decreasing at high nitrogen content. As the barrier height decreases, a small increase has been observed in the reverse bias current (Figure 1). However, forward bias current has decreased because of the defects in the interfacial layer and the increase in the resistance of the sample due to the impurity carriers. Observation of samples containing low nitrogen seems to be due to doping at the first glance but with increasing nitrogen concentration, the localize energy level in the optical band gap which behaves as deep-charge trapping centers are increased and sample tend to be insulator.

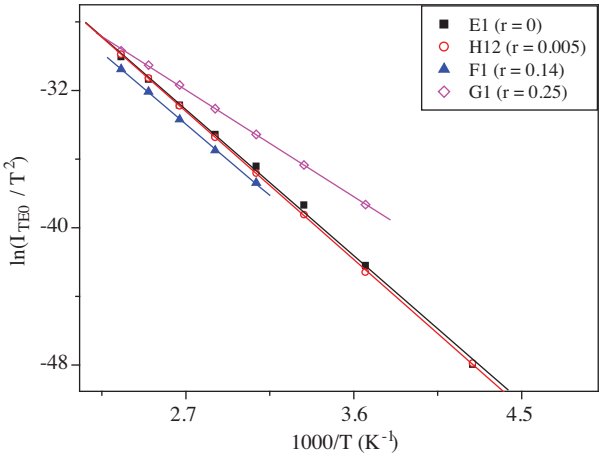

Figure 5. Thermionic emission saturation current characterized against temperature for samples with different nitrogen content.

Table 2. Modified Richardson constant and barrier height values which are calculated from plot of $\ln(I_{TE0}/T^2)$ versus 1000/T graph for case η=1.

Samples	r	η=1 case	
		A^* (A/K^{2}m^2)	ϕ_{BO} (eV)
E1	0	461	0.816
H12	0.005	598	0.828
F1	0.14	104	0.796
G1	0.25	1.47	0.595
J1	0.50	-	-

We made use of the Cheung method to calculate the series resistance of our samples. The dominant current mechanism is TE at room temperature and above. From Equation 5, the slope of the $dV/d(\ln(I))$

versus I graphs for different temperatures where ideality factor is kept 1 or close to 1 are given for sample H12 (Figure 7). As seen the Figure 7, the slope of the the $\mathrm{d}V/\mathrm{d}(\mathrm{In}(I))$ versus I curve has increased with decreasing temperature. It means that the series resistance increases as the temperature decreases. This suggests the series resistance can be empirically characterized over temperature for samples with different nitrogen content. Figure 8 shows the results of just such a characterization, showing the series resistance decreases exponentially as the temperature increases; and that in low nitrogen content series resistance decreases while it increases at high nitrogen content. In addition, due to the fact that the sample behaves like an insulator, no series resistance has been calculated at very high nitrogen content. Table 3 compares the series resistance at room temperature with the bulk resistance (R) values obtained by Current-Temperature (I-T) measurement in dark and at constant voltage. Although the series resistance values are high, it can be ignored when it is compared with the bulk resistance of the sample.

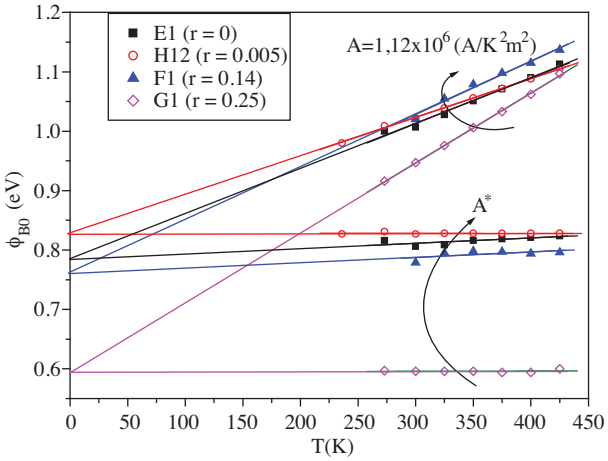

Figure 6. Temperature dependence of barrier height for samples with different nitrogen content.

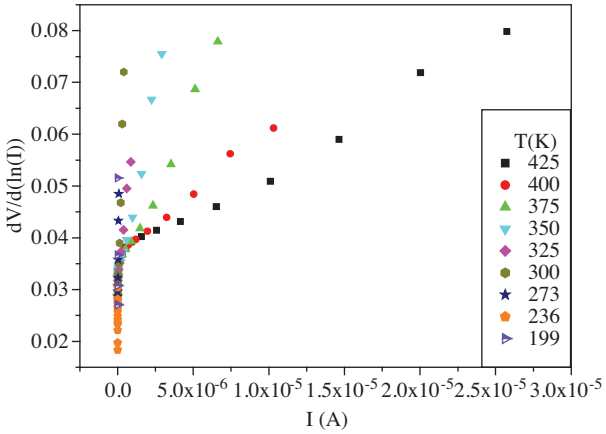

Figure 7. Temperature dependence of $dV/d(In(I))$ versus I curves for sample H12.

As the dominant current mechanism is TE, the series resistance and barrier height can be found by using Equation 6 from $H(I)$ versus I graph. The barrier height, which is found from plots of $\ln(I_{TE0}/T^2)$ versus $1000/T$ and $\ln(I)$ versus V at $T = 300$ K, have been contrasted with the barrier height from the $H(I)$ versus I graph in Table 3.

As shown in Table 3, the barrier height differences, not due to the method. This difference is due to different of Richardson constant. The barrier height values which were calculated by using modified Richardson constant for three methods are approximately same. However, the barrier height value calculated by the taken Richardson constant from the literature for n type crystal Si semiconductor is greater than the other calculations.

The a-SiN$_x$:H samples exhibit photoconductive behavior that increases even with a small increase in nitrogen content while it decreases at high nitrogen content [14]. The effect of this feature on the Schottky barrier has been investigated by conducting I-V measurements under different light intensity for all samples. As seen Figure 9, there is increase in the reverse and forward bias currents as the intensity of light increases for sample E1. This increment is up to a five-fold increase for reverse bias at low nitrogen content ($r \leq 0.14$), while it remains between one or two times for forward bias. There is, however, little difference between reverse and forward bias currents as the intensity of light increases for high nitrogen content alloys samples ($r \geq 0.25$).

Figure 10 gives the change in photoconductivity for all nitrogen alloyed samples under different light intensity and fixed reverse bias voltage. According to this, it is recognized that the diodes prepared at unique and low nitrogen content can be used as light-intensity receiver detector by using their I-V reverse bias behavior.

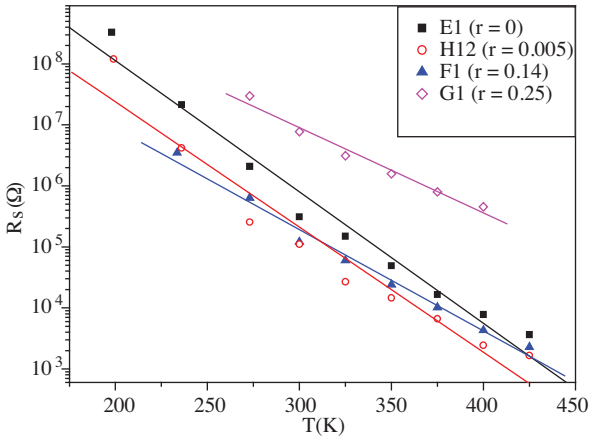

Figure 8. Temperature dependence of series resistance for samples with different nitrogen content.

Table 3. The values of barrier height and series resistance obtained by using different methods for all the samples in the η=1 case.

Samples		**E1**	**H12**	**F1**	**G1**	**J1**
r		0	0.005	0.14	0.25	0.50
R_S (dV/d(ln(I)) = f(I)) A*(from Table 2), T=300 K	kΩ	312±14	110±7	121±8	7750±85	
R_S ($H(I) = f(I)$) A*(from Table 2), T=300 K	kΩ	370±11	108±4	170±5	9600±35	
R, for forward bias T = 300 K (ln(I) = f(1000/T))	MΩ	2.3	1.1	1.87	41500	20000
R, for reverse bias T = 300 K (ln(I) = f(1000/T))	GΩ	66.5	160	30.8	4.8	57
$\phi_{BO}(I_{TE0}/T^2 = f(1000/T))$ A*(from Table 2), (η=1)	eV	0.816±0.013	0.828±0.003	0.796±0.010	0.595±0.005	
ϕ_{BO}(ln(I) = f(V)) T=300 K A*(from Table 2)	eV	0.806±0.014	0.827±0.014	0.779±0.010	0.596±0.006	
ϕ_{BO} (ln(I) = f(V)) A = 1.12×10^6 A/m^{2}K^2	eV	1.007±0.007	1.022±0.007	1.020±0.005	0.947±0.004	
ϕ_{BO} ($H(I) = f(I)$) A*(from Table 2), T=300 K	eV	0.827±0.001	0.850± 0.001	0.809±0.001	0.596±0.001	

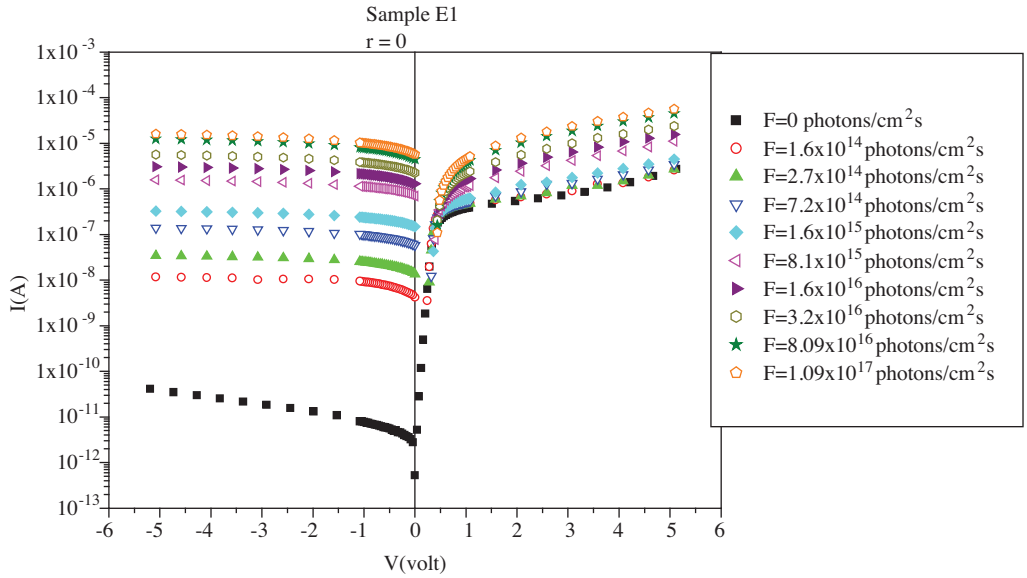

Figure 9. Current voltage characteristic of pure sample under taken different light intensity (F, photons/cm^2 s) at room temperature.

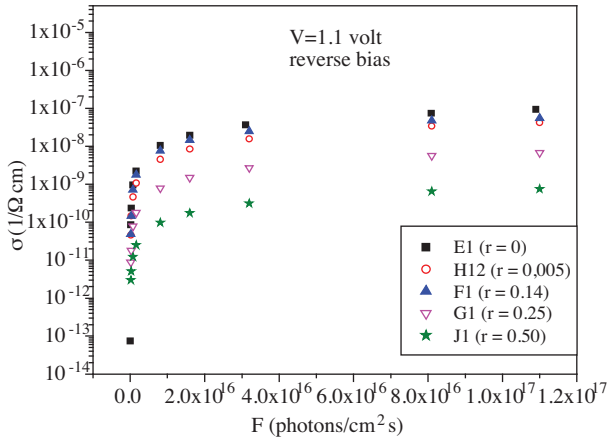

Figure 10. Light intensity dependence of photoconductivity (σ) for all nitrogen alloyed samples in room temperature and fixed reverse bias ($V = 1.1$ V).

C-V characteristics of amorphous semiconductors are different from crystals due to the fact that there is no orderly structure in amorphous structures to localize energy levels in the optical band gap. In amorphous structures, the defects close to the Fermi energy show similar behavior to the deep centers of crystal structure and the depletion region is limited to the size of the defect density. Therefore the change in the capacitance with changing voltage value may not be observed in samples with high defect density. Figure 11 show that the C-V change at fixed frequency for samples with different nitrogen content. To eliminated the little change of the depletion region while taken C-V measurements, we select the $f = 1$ MHz. According to this, capacitance has remained stable between ± 5 V intervals and it has decreased with high nitrogen content. In this case, the

samples behave like insulator and the capacitance is given with the following equality

$$C = \varepsilon_0 \varepsilon_r \frac{S}{d}. \tag{8}$$

Here, S denotes area; d denotes sample thickness; and ε_0 and ε_r are the electrical permeability in free space and the dielectric constant of the sample, respectively.

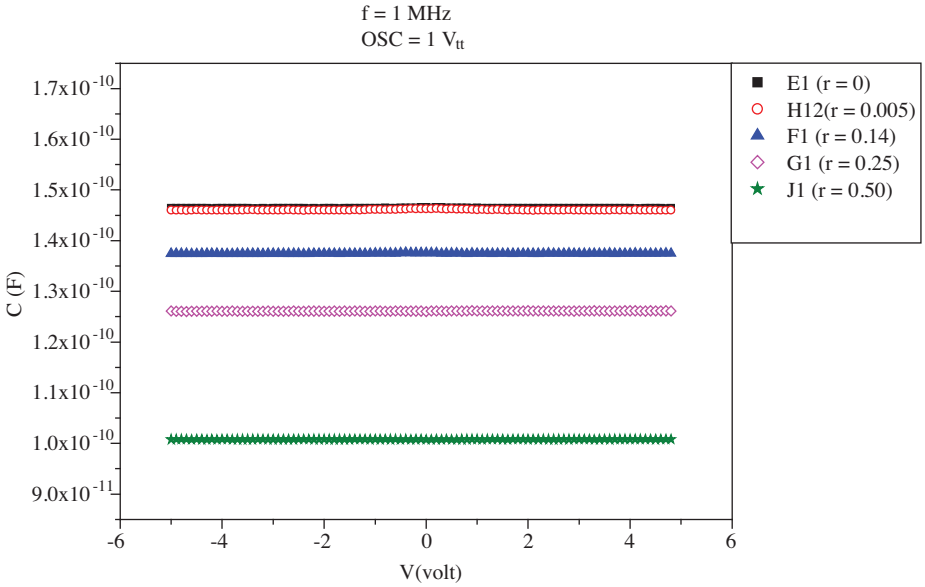

Figure 11. Capacitance Voltage characteristic of samples with different nitrogen content in room temperature and fixed frequency ($f = 1$ MHz).

Figure 12 shows the dielectric constant has been calculated from the Equation 8 for samples with different nitrogen content. According to this, as the content of nitrogen has increased, the dielectric constant has decreased.

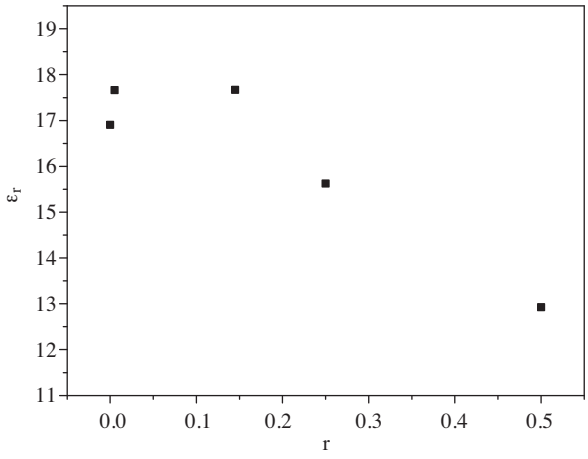

Figure 12. Dielectric constant as a function of nitrogen content ($f = 1$ MHz, OSC $= 1$ V_{tt}).

The optical parameters of the samples (such as thickness d, breaking indices n, and optical band space E_g) have been found by using Swanepoel method [15, 16]. The change in the optical parameters according to the nitrogen content has been shown in Table 4.

Table 4. Optical parameters of all samples.

Samples	r	E_g (eV)	n (λ = 700 nm)	d (μm)
E1	0	1,68	3,56	1,15
H12	0.005	1,68	3,63	1,21
F1	0.14	1,68	3,48	1,29
G1	0.25	1,75	3,21	1,24
J1	0.50	1,92	2,42	1,28

As is known, the relationship between refractive index and dielectric constant is $n = \sqrt{\varepsilon_r \mu_r}$ where μ_r are the magnetic permeability. As seen Table 4, the refractive index is decrease with increasing nitrogen content. Hence, ε_r decreased with the increase in the rate of nitrogen is an expected result.

4. Conclusion

As district from crystal Schottky diodes, forward bias current of Mg/a-SiN$_x$:H/Au structures have been saturated at $V \geq 1$ volt. However, for small values of voltage ($V < 1$ volt), these samples behaves like crystal Schottky diodes.

At the first glance samples containing low nitrogen concentration seems to be as doping, but the diode characteristic is deteriorated with increasing nitrogen concentration and it is tend to be insulators. Because of the fact that the density of localize energy levels in the optical band gap which are behaves as deep-charge trapping centers is increased with increasing nitrogen concentration. As a result, due to the increasing nitrogen content, I_f / I_r ratio has decreased and the I_f / I_r ratio has reached unity in highly nitrogen content alloys samples.

The dominant current mechanism in room and over the room temperatures is thermionic emission. Therefore, barrier height and modified Richardson constant calculations can be made by using the I-V measuring taken from this temperature range (300–420 K). In lower temperatures, in some of the samples, tunneling current is dominant.

While thermionic emission is dominant in lightly nitrogen alloyed samples, the tunneling current mechanism becomes dominant as the content of nitrogen increases. This behavior is expected for materials which become more insulated as increases the content of nitrogen.

Calculation of the ideality factor correctly minimizes the possible errors in the modified Richardson constant and barrier height calculations. The barrier height values, which were calculated by using a modified Richardson constant for three methods, are approximately same. However, the barrier height value calculated by the taken Richardson constant from the literature for n-type crystal Si semiconductor is greater than those for other calculations. In addition to the barrier height obtained by using the Richardson coefficient A found in literature for n-type crystal Si semiconductor, the increase is found to parallel the temperature abscissa. However the barrier height calculated by using the modified Richardson constant A^* is independent of temperature. The

lines drawn in accordance to with those two behaviors meet at zero Kelvin.

Considering the modified Richardson constant and the change in barrier height with the different nitrogen content in Mg / a-SiN$_x$:H / Au structures, both parameters have increased by a very small amount with the increase of the nitrogen content. While both parameters have rapidly decreased as the nitrogen content increased. The decrease in barrier height has resulted in increase of the reverse bias current while forward bias current has decreased due to the increase in the resistance of the sample resulting from the increase of the nitrogen content. Indistinguishably the series resistance decreases in samples with low nitrogen content compared to the pure sample while it increases as the content of nitrogen increased.

In all prepared samples, forward and reverse bias currents have tended to increase under illumination. This increase reached a factor of five increase for reverse bias in lightly nitrated content alloys samples ($r \leq 0.14$), while it remained between one and two times for forward bias. In highly nitrogen content alloys samples ($r = 0.50$), there is only little change in reverse and forward bias currents as the intensity of lighting increases. Thus, it is found out that, using the reverse bias I-V behavior of the diodes obtained from pure or lowly nitrated samples, they can be used as detectors measuring the intensity of light. The Schottky barrier made from the crystal semi-conductors has shown that this behavior observed in pn junction diodes is also valid for amorphous semiconductors.

In amorphous semiconductors, due to the fact that there is not an orderly structure and that there is a localized energy level in the optical band gap, C-V characteristics are different from those of the crystals. The capacitance is fixed at $\pm$5V for all the samples. At low nitrogen content ($r \leq 0.14$), the capacitance increased while it rapidly decreased with the increase in the nitrogen content ($r > 0.14$). Therefore, the dielectric constant increases in lightly nitrogen content alloys samples ($r \leq 0.14$), it decreases with the increase of the nitrogen content ($r > 0.14$). The same behavior is also observed in the fracturing index of the samples.

Acknowledgements

The work is supported by TÜBİTAK Research Grant 104T123 and Hacettepe University Research Grant 0401602006.

References

[1] H. Kakiuchi, Y. Nakahama, H. Ohmi, K. Yasutake, K. Yoshii, Y. Mori, *Thin Solid Films*, **479**, (2004), 17.

[2] I. Kobayashi, T. Ogawa and S. Hotta, *Jpn. J. Appl. Phys.*, **31**, (1992), 336.

[3] J. C. Barbour, H. J. Stein, O. A. Popov, M. Yoder and C. A. Outten, *J. Vac. Sci. Technol.*, **A9 (3)**, (1992), 480.

[4] M. J. Powell, B. C. Easton, and O. F. Hill, *Appl. Phys. Lett.*, **38**, (1981), 794.

[5] A. J. Lowe, M. J. Powell and S. R. Elliott, *J. Appl. Phys.*, **59**, (1986), 1251.

[6] H. Matsuura, T. Okuno, H. Okushi, S. Yamasaki, A. Matsuda, N. Hata, et al. *Jpn. J. Appl. Phys.*, **22**, (1983), L197.

[7] L. Magafas, N. Georgoulas and A. Thanailakis, *Microelectronics Journal*, **28**, (1997), 107.

[8] S. S. Georgiev, A. Toneva, D. Sueva, *Solar Energy Materials & Solar Cells*, **58**, (1999), 387.

[9] I. Ay and H. Tolunay, *Solid-State Electronics*, **51**, (2007), 381.

[10] D. Donoval, M. Barus and M. Zdimal, *Solid-State Electronics*, **34**, (1991), 1365.

[11] D. Donoval, V. Drobny and M. Luza, *Solid-State Electronics*, **42**, (1998), 235.

[12] S. M. Sze, *Semiconductor Devices Physics and Technology*, (John Wiley & Sons, New York. 1985), p. 93.

[13] S. K Cheung and N. W. Cheung, *Appl. Phys. Lett.*, **49**, (1986), 85.

[14] I. Ay and H. Tolunay, *Solar Energy Materials & Solar Cell*, **80**, (2003), 209.

[15] I. Ay and H. Tolunay, *Turkish Journal of Physics*, **25**, (2001), 215.

[16] R. Swanepoel, *J. Phys. E: Sci. Instrum.*, **16**, (1983), 1214.